Molecular Description of Grafted Supramolecular Assemblies on Gold Surfaces: Effect of Grafting Points and Chain Lengths

Ludovic Garnier, Christine Bonal, Patrice Malfreyt

Molecular description of grafted supramolecular assemblies on gold surfaces: effect of the grafting points and chain lengths

Ludovic Garnier, Christine Bonal,* and Patrice Malfreyt

Université Clermont Auvergne, CNRS, SIGMA Clermont, Institut de Chimie de Clermont-Ferrand, F63000, Clermont-Ferrand, France.

E-mail: christine.bonal@uca.fr
Phone: +33 (0)4.73.40.72.04. Fax: +33 (0)4.73.40.53.28

Abstract

The association of the 4 aminoazobenzene (4AA) by two different water-soluble hosts, β-Cyclodextrins (β-CD) and calixarenesulfonates (CnS), was studied in heterogeneous conditions using molecular simulations. This situation is achieved by immobilization of macrocycles onto a gold Au (111) surface. Severals factors that can influence the binding properties are investigated here through the chain length of alkylthiols spacer of the surface-immobilized host and the number of attachments points to the surface. A conformational change of β-CD as a function of the chain length is evidenced upon grafting on the gold surface whereas CnS does not show any changes. It is then possible to tune the thermodynamic properties of β-CD by changing the grafted chain length and forming a larger hydrophobic region. The mechanisms of insertion of the guests into the cavities are similar to those obtained in homogeneous system. Whereas the 4AA is included longitudinally in the β-CD cavity, it interacts rather with the sulfonate groups at the outer edge of the cavity.

1 Introduction

Supramolecular chemistry is based on all types of intermolecular interactions that include non-covalent interactions such as electrostatics, hydrogen bonding, van der Waals and hydrophobic interactions. A large body of work has been reported in this field over the past thirty years (since the 1987 Nobel Prize[1–3]). Macrocycle hosts and suitable hosts can form host-guest inclusion complexes with high binding affinities in aqueous solution. The families of cyclodextrins (CDs)[4] and calixarenes[5] are among the most important organic supramolecular hosts. Cyclodextrin derivatives mainly serve for drug solubilization and delivery thanks to their properties such as inexpensive, available on an industrial scale and being safe.[6] Calixarenes can be easily modified and consequently are mainly used for the building of functional supramolecular architectures.[7] Azobenzene is a guest molecule of particular importance to obtain driven molecular machines,[8 9] such as photoregulated host-guests macroscopic objects using the differential affinities of hosts for the trans-azobenzene and cis-azobenzene[10]

More recently, we have investigated the association of water-soluble macrocyclic hosts with 4-aminoazobenzene (4AA) in water using both experimental and atomistic simulation approaches,[11].[12] Using UV-visible spec-

troscopy, we have obtained the whole thermodynamical characterization of the association between hosts (β-Cyclodextrins and calixarenesulfonates) with 4AA guest. These thermodynamic studies have been developed by molecular dynamic simulations using the potential of mean force technique (PMF). Our combined approach has provided a structural and energetic characterization of these complexes in solution.

The passage of host-guest chemistry from solution to solid surface becomes a fundamental requirement for the development of applications in various fields including biology, nanotechnology, environmental and energy technologies.[13] However, many molecular devices operate well in solution but that are no longer effective when transferred onto a solid surface.[14–16] As an example, the photocontrolled molecular shuttles formed from the host-guest chemistry between alpha-CD and azobenzene derivatives exhibit such behavior.[10] Moreover, it is now accepted that the association process of supramolecular assemblies[17] can be different between homogeneous (free in solution) and heterogeneous conditions (host or guest grafted on surface) in water. Concerning the association between CDs and some guests totally inserted into the host cavity, a higher association constant at the surface than in solution was typically measured.[18–21] The same conclusions have been drawn with the association of ferrocenemethanol with gold confined CD by using molecular simulations. The larger negative enthalpy change obtained for the surface was attributed to the wider opening of the surface confined CD leading to an insertion of a larger numbers of atoms.[21] Clearly, changing the surrounding environment of operation from solution to solid surface affects the structure of assemblies of molecule and therefore the binding properties.

Molecular dynamic simulations has demonstrated that it can access the structure of host-guest systems in heterogeneous conditions in water. We take the route of investigating two hosts : a β-cyclodextrin (CD) and a *p*-sulfonatocalixarenes (C4S and C6S) (see Figure 1). These hosts are then grafted on a gold surface through sulfur atoms as shown in Figure 1. The gold surface was chosen because this metal substrate is the most widely studied for self-assembled monolayers (SAM) preparation and offers a large spectrum of applications in nanoscience and nanotechnology[22] such as chemical sensors, lubricating layers or corrosion inhibitors. At the gold-sulfur interface, the covalent interaction requires formation of gold-thiolate (RS-Au) bond(s). The sulfur-metal interfacial chemistry has been investigated by numerous techniques such as scanning tunnelling microscopy (STM), low-energy electron diffraction (LEED) and X-ray spectroscopic techniques and first principle calculations.[23,24] The reader is redirected to significant works in this field.[22,25–28] Different binding modes have been suggested for the S-Au bond[25,26] : a classical view involving a monothiolate bonding on an Au atom of the Au (111) surface, a disulfide bonding, a complex involving an Au adatom and a thiolate (Au-SR), and a polymeric chain structure where monothiolates are bridging Au adatoms. In addition, the transport of Au adatoms at the interface leads to the breaking and making of Au-S bonds.[24]

Since the sulfur-gold chemistry is complex in terms of diversity of the adsorption sites, binding, presence and transport of Au adatoms, we take the route of defining a model system : an Au (111) gold surface in which only the chain length of alkylthiols spacer of the surface-immobilized host and the number of grafting points involving the formation of covalent thiolate-Au (S-Au) bonds with the substrate will vary. We assume that the variety of the Au-S bonding will be implicitly considered through the number of grafting points. Actually, it has been reported that the inclusion properties can depend of these key-parameters. Previous work has indeed shown that difference in the heterogeneous binding of Mg^{2+}, Ca^{2+} and Sr^{2+} ions has been obtained for similar ligands that are differently attached onto a Au (111) surface through one or two arms.[29]

Inspired by these results, herein we report the structure of the complexes in heterogeneous conditions as a function of both the chain length linked to the surface (that is symbolized in the paper by the letter **l**) and the number of an-

chors points (symbolized by **a**). Thus, an inclusion complex of (2a7l) corresponds to a system with two attachments points and a chain length of seven. We only investigate the protonated form of the 4AA since it was shown from experiments[11,30] and simulations[11,12] that stable complexes with calixarene were found at acidic pH and no inclusion of the guest into the calixarene at neutral pH. For the β-cyclodextrin, the association was identical at the two pH conditions. As a conclusion, the simulations reported here are performed in acidic solutions.

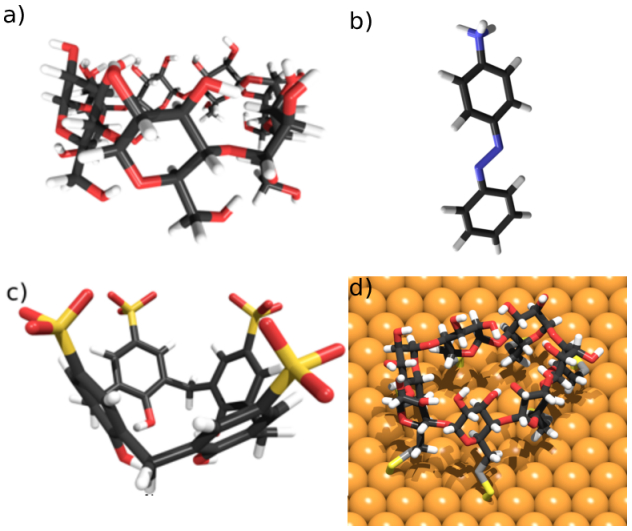

Figure 1: Representation of a) free β-CD; b) a protonated 4AA; c) *p*-sulfonatocalix[4]arene and d) grafted β-CD.

2 Results and discussion

In order to deeply examine the architectures of these complexes grafted onto the gold surface at the molecular scale as a function of the number of attachments points and length of the grafted chains, we first examined the displacements in the x and y directions of the chains attached to the Au surface. For clarity, we focus only on (β-CD, 4AA). Plots of displacements for all others systems are given in supplementary information (see Figure S4). Figures 2a and 2b represent the displacement of the β-CD for 2 (**2a**) and 7 (**7a**) anchor points as a function of the grafted chain length (from **1l** to **7l**).

As expected for a given chain length, we observe that the mobility of the chain decreases

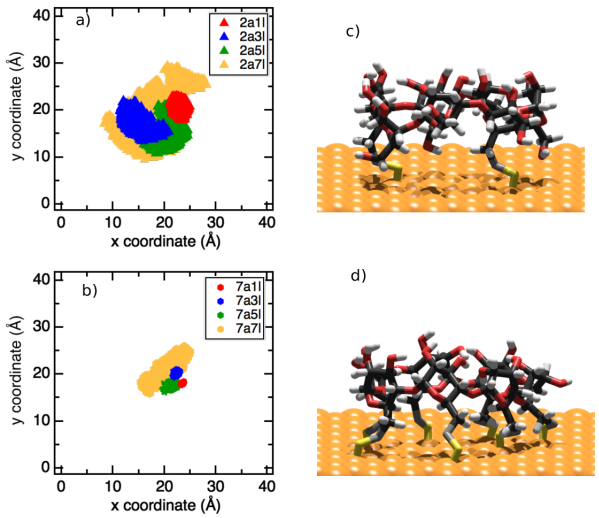

Figure 2: a) and b) Mean displacement of the β-Cd on the gold surface along x and y coordinates as a function of both the number of anchor points (**a**) and the length of the grafted chains (**l**). Representations of the β-Cd grafted with c) 2 anchor points and d) 7 anchor points.

as the number of interaction points increases. Actually, for the largest chain investigated here (**7l**), the grafted host can sample a region of 20 Å in the x and y directions with 2 anchor points (see Figure 2a). This sampled space in the x and y directions is reduced to 10 Å with 7 anchor points (see Figure 2b). The chain length also impacts on the mobility. Indeed, increasing the chain length from (**1l**) to (**7l**) leads to increase the displacements in the x and y directions by a factor 4 (see Figures 2a and 2b).

To further analyze the structural properties, we also examine in Figure 3 the size of the wide (upper) and narrow (lower) rims of the grafted macrocycle as a function of the length of the grafting chains and number of anchor points. Clearly, the length of the grafted chains impacts the conformation of the β-CD to a greater extent than CnS (Figure 3a). We observe a large distortion of the narrower rim of the β-CD with a change in the size of about 1 Å for the shortest chain length (**1l**). For this latter system, the size of the lower rim is larger than that of the upper rim. β-CD therefore undergoes a significant deformation. The size of the lower rim becomes comparable again to that obtained in homogeneous medium when the length of the

grafted chain is large, here (**7l**). Finally, the number of grafting points has little influence on the shape of the β-CD.

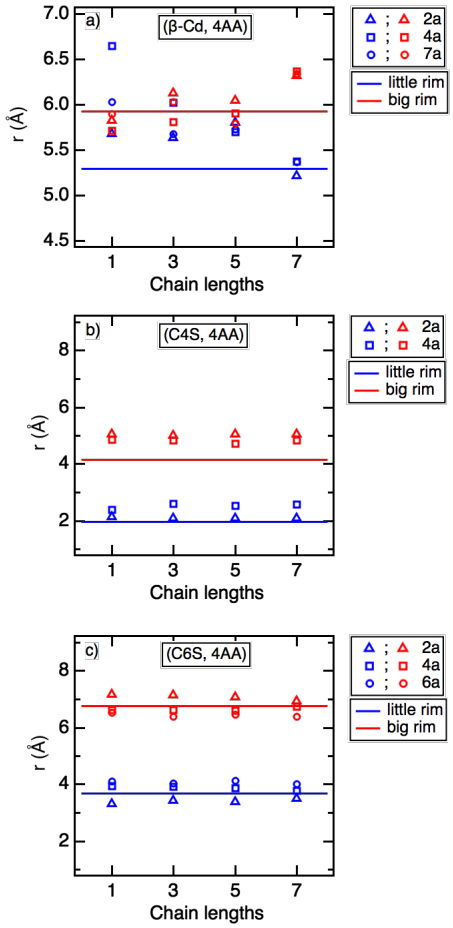

Figure 3: Cavity radius of the wider and narrower rims of hosts depending of the length of grafted chains in: a) β-Cd; b) C4S and c) C6S. The blue and red lines correspond to the size of the wider and narrower rims of the macrocycles in homogeneous phase.

The fact that few changes are observed as a function of the chain length with CnS is evidenced in Figure 3b. Indeed, we obtain the same value of the cavity radius for all chain lengths for a given value of anchor point. Nevertheless, the size of C4S cavity seems to be dependent on the value of **a**. In the case of (C4S, 4AA) with two anchoring points, the size of the upper rim is larger than that obtained in homogeneous conditions. For the same system with four anchoring points, the sizes of both rims are increased significantly. Note that this dependence is less marked in C6S (see Figure 3c).

In summary, all these results about the conformational change of the cavities highlight that the passage of host-guest chemistry from solution to solid surface has a greater effect on β-CD than on CnS. This is in line with the expected greater flexibility of the β-CD and a deeper insertion of 4AA helped by a larger cavity size. This aspect should have an important role in the insertion of the guest.

In order to address the aspect of insertion, we show in Figures 4a and 4b two typical conformations of inclusion (β-CD, 4AA) complexes for two chain lengths (**1l** and **7l**) and the largest number of grafted points (**7a**). Figure 4c shows an insertion rate ranging from 40% to 60% into the β-CD cavity. This type of insertion does not seem to be too impacted by the key-parameters of this study, *i.e*, the number of grafting points and the chain length. The comparison with the insertion rate calculated in bulk water phase confirms this conclusion. However, when we consider the insertion no longer in the cavity of the β-CD but in the hydrophobic region extended to the grafted chains, the values of insertion are significantly changed as illustrated in a conformation in Figure 4b and quantified in Figure 4d.

Interestingly, increasing the grafted chain length changes significantly the insertion of the guest into the region delimited by the cavity and the grafted chains. Insertion rates of the order of 90% to 100% are obtained for the longest chains demonstrating that the insertion in the β-CD of the 4AA is largely favored with longer grafted chains. Since the association in inclusion complexes is proportional to the number of inserted atoms, we can expect a more favorable association when increasing the grafted chain length. A grafted chain length of 7 carbons is optimal to obtain a total insertion of the guest. For this grafted chain length, the host-guest van der Waals interaction is about - 130 kJ mol^{-1} against -90 kJ mol^{-1} in homogeneous conditions whereas the electrostatic contribution is about - 40 kJ mol^{-1} for both cases. In the case of two anchoring points (**2a**) and the longest chain length (**7l**), we observe that the percentage found is lower than in other cases.

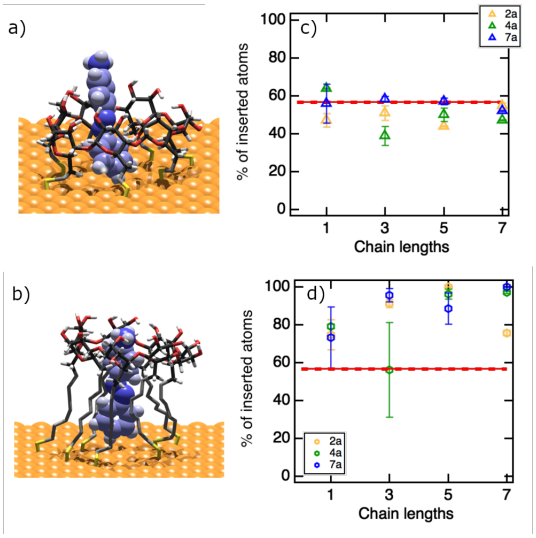

Figure 4: Conformations of (β-CD, 4AA) for a) **7a1l** and b) **7a7l**. Percentage of 4AA atoms inserted c) into the β-CD cavity and d) into the cage composed of the cavity and the region of grafted chains. The red lines correspond to the insertion calculated in bulk water phase

.

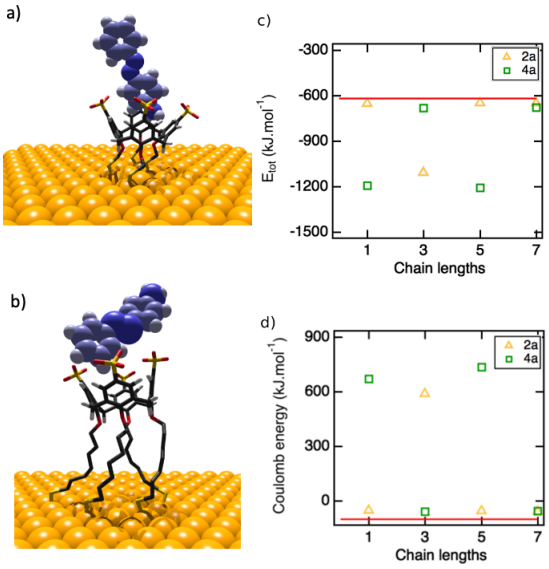

Figure 5: Conformations of the complex formed by C4S and protonated 4AA for 4 grafting points qnd two grafted chain lengths a)$l = 1$ and b)$l = 7$; c) Total energy (kJ mol^{-1}) between C4S and 4AA; d) Electrostatic contributions (kJ mol^{-1}) between 4AA and water molecules within a radius of 14 Å.

In fact, with few number of attachments points on the surface, the macrocycle has more freedom of movement. Consequently, it can move along the x, y and z axes. The chain can then tilt toward the surface which drastically hinders the insertion of the 4AA into the host cavity. A representation of this case is given in the Supporting Information (see Figure S5).

We now turn our attention to the association between C4S and the protonated 4AA guest. The equilibrium conformations of theses structures at 4 grafting points are represented on Figures 5a and 5b for the smallest (**4a1l** and largest **4a7l**) grafted chains. In Figure 5c, we have represented the total energy contributions (sum of the Lennard-Jones and electrostatic energy parts) between the host and the guest molecules. The red curve represents the same contribution in homogeneous systems.[12] The total energy values may be either identical or significantly more favorable to those obtained in the homogeneous system. The decomposition into the Lennard-Jones (LJ) and electrostatic contributions are given in supplementary information in Figure S6. Contrary to what we have observed for the association between β-CD and 4AA, the LJ contribution is less favorable but the electrostatic contributions are much more favorable by ranging from -600 to -1200 kJ mol^{-1} (see Figure S6b). As confirmed in Figure S6a in the Supporting Information by the insertion rate, this indicate that the insertion of 4AA is much less marked and that 4AA interacts more strongly with the sulfonate groups of C4S through electrostatic interactions. The association between C4S and 4AA is mainly governed by the electrostatic interactions.

In addition, significant differences in the total energy contributions (and consequently in the electrostatic interactions) are observed in Figure 5c as a function of the number of grafting points. For instance, for **2a5l** the total energy between C4S and 4AA is about $-600\,\mathrm{kJ\,mol^{-1}}$ whereas the same contribution is in the order of $-1100\,\mathrm{kJ\,mol^{-1}}$ for **4a5l**. This result reveals two modes of inclusion of the host that are energetically equivalent. Indeed, we can see in Figure 5d that the total energy contribution between C4S and 4AA is counterbalanced by the electrostatic contributions between 4AA

and water molecules. To characterize these two modes of binding, we have calculated a parameter α that specifies the position of the amine function of 4AA with respect to phenyl groups of C4S (the definition of α is given in supplementary information in Figure S7). Value of $\alpha < 1$ corresponds to the insertion of the phenyl group whereas $\alpha > 1$ to that of the protonated amine. The results obtained for α for different values of **a** and **l** are given on Figure 6a. For a same chain length, α can be greater or smaller than 1, indicating thus that the two inclusion modes occur. Let us recall that for the same system in homogeneous conditions, a privileged penetration of the phenyl part of the 4AA rather than the amino group has been established.[12] However, note that a scan of the literature data regarding water-soluble calixarenes and quaternary ammonium cations also reports a non-selective insertion of the aromatic derivative or ammonium cation into the cavity.[31]

Since favorable electrostatic interactions between C4S and 4AA may be partly related to the possibility of forming hydrogen bonds between the two species, we have investigated the formation of these H-bonds. The H-bonds between water and the 4AA amine group have been reported in Figure 6b and those between sulfonate groups and the 4AA amine group in Figure 6c. As expected, the insertion of the phenyl group into the host cavity ($\alpha < 1$) prevents any possibility of H-bonds (Figure 6c) between the protonated amine and the sulfonate groups due to the large separation distance. However, this situation allows to enhance the hydrophobic interactions of the guest with C4S. It is noteworthy that this orientation of the guest upon complexation leads to a less favorable electrostatic term between C4S and 4AA counterbalanced by a less unfavorable electrostatic contribution between 4AA and water molecules (see Figure 5c and Figure 6a). In contrast, the electrostatic term is largely negative for $\alpha > 1$ corresponding to the penetration of the protonated group into the host cavity. This results in a loss of H-bonds between 4AA and water and more unfavorable (4AA..water) electrostatic contributions (see Figure 5d).

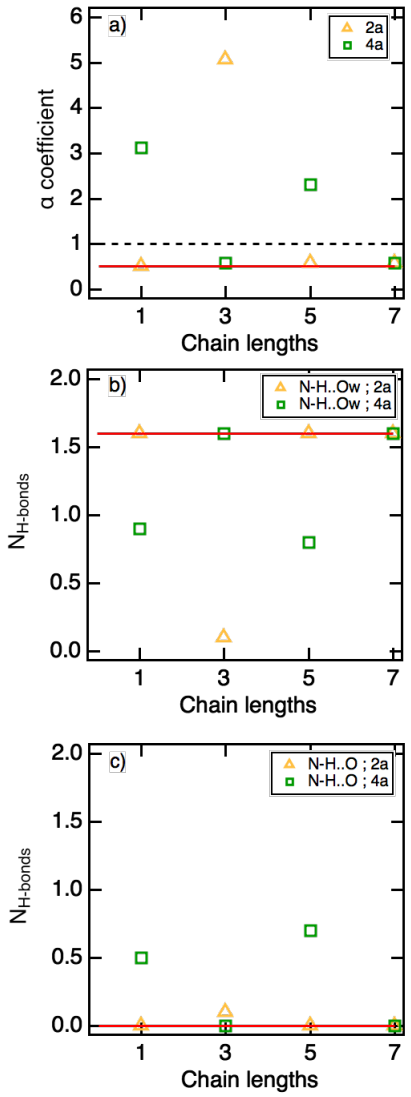

Figure 6: a) α coefficient values in (C4S,4AA) complex as a function of grafted chain length and number of grafting points ; b) number of hydrogen bonds between water and the 4AA amine group ; c) number of ydrogen bonds between sulfonate groups of C4S and the amine group of 4AA.

3 Conclusion

The association between two grafted macrocyclic hots (β-CD and C4S) and the protonated 4AA has been investigated in terms of the dependences of the insertion rate and energy contributions on the number of grafting points and grafted chain length. The results were compared with the associations in bulk water phases. First, an in-depth analysis of the association process at the molecular level

has shown that the grafted chain length can impact the insertion rate of 4AA into β-CD and as a consequence the strength of the interaction between the host and guest. Actually, the longest chain length of alkylthiols spacer of the surface-immobilized host induces a large expansion of the hydrophobic zone and consequently allows a more deeply insertion of the 4AA into the host cavity. On the other hand, for the shortest chain length the association will probably be less favorable than in the homogeneous phase due to the presence of the surface. Second, the association of 4AA with C4S is much weaker with a very weak dependence of grafting parameters on the association. We establish a non-selective insertion of 4AA into the host cavity (by the aromatic moities or by the protonated amine). The 4AA interacts with C4S via two modes of binding which are energetically equivalent.

4 Computational methods

The simulation boxes contain one protonated 4AA molecule (Figure 1b), one host molecule (C4S or β-CD), an Au (111) gold surface and 2000 water molecules. The grafted hosts are immobilized on a five-layer Au(111) surface through the seven sulfur atoms. Since the system is nonperiodic along the direction normal to the surface (z axis), the simulation cell is closed by an additional gold layer. To keep applying the periodic conditions in the three dimensions and a three-dimensional method for the calculation of the long-range electrostatic interactions (PPPM 3D), we add 248 Å of void above the top gold layer.[32] The boxlengths along x, y and z directions are 40, 40 and 300 Å, respectively. In acidic solution, all the sulfonate groups located on the upper rim are deprotonated.[11] Depending on the host, some ions such as Cl^- or Na^+ can be added to maintain the neutrality of the simulation box. The details of the grafting methodology are given in supplementary information S1.

Concerning the force fields, we chose the TIP4P2005 model for water molecules,[33] and the General AMBER Force Field (GAFF) for hosts and guests molecules.[34] However, for the guest molecule the dihedral angle C-N=N-C was taken from the work of Heinz *et al.*[35] and the force field for the S-Au bond was taken from reference[36] .

MD simulations were performed with the LAMMPS package.[37] To constrain H based bonds and the HOH angle for water we used the SHAKE algorithm.[38] The Lennard-Jones crossing parameters were calculated using Lorentz-Berthelot rules (i.e $\epsilon_{ij} = \sqrt{\epsilon_{ii}\epsilon jj}$ and $\sigma_{ij} = \frac{\sigma_{ii}+\sigma_{jj}}{2}$ where i and j refer to the force centers and ϵ and σ are the energy parameter and diameter of atoms of types i and j, respectively.). Our simulations were carried in the constant NVT ensemble with the velocity-verlet integrator and a timestep of 2 fs. The Langevin[39,40] thermostat was used with a relaxation time of 2 ps to keep the temperature at 300K. Both long-range electrostatic interactions and long-range dispersion-repulsion tail correction[41] were considered. PPPM style (particle-particle particle-mesh) with a relative error force of 10^{-4} was used to calculate the long-range electrostatic interactions. This method maps atom charge to a 3D mesh.[42,43]

As mentioned in the introduction the chain length (**l**) and the number of anchor points (**a**) are two key-parameters under investigation in this paper. This implies that several simulations were performed to study various anchor points and chain lengths. In the table 1 we summarized these parameters. Each simulation was composed of an relaxation phase (NVE ensemble) of 10 ps and an equilibrium phase (NVT ensemble) of 1.4 ns. Finally the thermodynamic and structural properties were averaged over 20 ns of the acquisition phase in the NVT statistical ensemble.

Table 1: Parameters for the grafted hosts

Association	Nb of anchor points	Chain length
(β-Cd, 4AA)	2, 4 and 7	1, 3, 5 and 7
(C4S, 4AA)	2 and 4	1, 3, 5 and 7
(C6S, 4AA)	2, 4 and 6	1, 3, 5 and 7

Supporting Information Available

The methodology of grafting the chains onto the gold surface, typical conformations of the different complexes, mean displacements, insertion rates, energy contributions and the definition of the α coefficient are provided.

References

(1) Pedersen, C. J. The Discovery of Crown Ethers (Noble Lecture). *Ang. Chem.* **1988**, *27*, 1021–1027.

(2) Cram, D. J. The Design of Molecular Hosts, Guests, and Their Complexes (Nobel Lecture). *Angew. Chem. Int. Ed.* **1988**, *27*, 1009–1020.

(3) Lehn, J.-M. Supramolecular Chemistry—Scope and Perspectives Molecules, Supermolecules, and Molecular Devices (Nobel Lecture). *Angew. Chem. Int. Ed.* **2018**, 89–112.

(4) Szejtli, J. Introduction and General Overview of Cyclodextrin Chemistry. *Chem. Rev.* **1998**, *98*, 1743–1754.

(5) Guo, D.-S.; Liu, Y. Supramolecular Chemistry of p-Sulfonatocalix[n]arenes and Its Biological Applications. *Acc. Chem. Res.* **2014**, *47*, 1925–1934.

(6) Ma, D.; Hettiarachchi, G.; Nguyen, D.; Zhang, B.; Wittenberg, J. B.; Zavalij, P. Y.; Briken, V.; Isaacs, L. Acyclic Cucurbit[*n*]uril Molecular Containers Enhance the Solubility and Bioactivity of Poorly Soluble Pharmaceuticals. *Nat. Chem.* **2012**, *4*, 503–510.

(7) Böhmer, V. Calixarenes, Macrocycles with (Almost) Unlimited Possibilities. *Angew. Chem. Int. Ed.* **1995**, *34*, 713–745.

(8) Patra, D.; Zhang, H.; Sengupta, S.; Sen, A. Dual Stimuli-Responsive, Rechargeable Micropumps via "Host–Guest" Interactions. *ACS Nano* **2013**, *7*, 7674–7679.

(9) Yamaguchi, H.; Kobayashi, Y.; Kobayashi, R.; Takashima, Y.; Hashidzume, A.; Harada, A. Photoswitchable Gel Assembly Based on Molecular Recognition. *Nat. Commun.* **2012**, *3*, 603.

(10) Yang, H.; Yuan, B.; Zhang, X.; Scherman, O. A. Supramolecular Chemistry at Interfaces: Host–Guest Interactions for Fabricating Multifunctional Biointerfaces. *Acc. Chem. Res.* **2014**, *47*, 2106–2115.

(11) Garnier, L.; Sarraute, S.; Israëli, Y.; Bonal, C.; Malfreyt, P. Associations of Water-Soluble Macrocyclic Hosts with 4-Aminoazobenzene: Impact of pH. *J. Phys. Chem. B* **2018**,

(12) Garnier, L.; Bonal, C.; Malfreyt, P. Thermodynamics of Supramolecular Associations with Macrocyclic Water-Soluble Hosts. *ACS Omega* **2019**, *4*, 16899–16905.

(13) Yang, Y.-W.; Sun, Y.-L.; Song, N. Switchable Host–Guest Systems on Surfaces. *Acc. Chem. Res.* **2014**, *47*, 1950–1960.

(14) Wang, P.; Hill, E. H.; Zhang, X. Interfacial Supramolecular Chemistry for Stimuli-Responsive Functional Surfaces. *Prog. Chem.* **2012**, *24*, 1–7.

(15) Kim, H. J.; Lee, M. H.; Mutihac, L.; Vicens, J.; Kim, J. S. Host–guest Sensing by Calixarenes on the Surfaces. *Chem. Soc. Rev.* **2012**, *41*, 1173–1190.

(16) W. Ludden, M. J.; N. Reinhoudt, D.; Huskens, J. Molecular Printboards: Versatile Platforms for the Creation and Positioning of Supramolecular Assemblies and Materials. *Chem. Soc. Rev.* **2006**, *35*, 1122–1134.

(17) Ghoufi, A.; Bonal, C.; Morel, J. P.; Morel-Desrosiers, N.; Malfreyt, P. Structures and Energetics of Complexes of the p-Sulfonatocalix[4]arene with Ammonium, Alkylammonium, and Tetraalkylammonium Cations in Water Using Molecular Dynamics Simulations. *J. Phys. Chem. B* **2004**, *108*, 5095–5104.

(18) Domi, Y.; Yoshinaga, Y.; Shimazu, K.; Porter, M. D. Characterization and Optimization of Mixed Thiol-Derivatized β-Cyclodextrin/Pentanethiol Monolayers with High-Density Guest-Accessible Cavities. *Langmuir* **2009**, *25*, 8094–8100.

(19) Rojas, M. T.; Koeniger, R.; Stoddart, J. F.; Kaifer, A. E. Supported Monolayers Containing Preformed Binding Sites. Synthesis and Interfacial Binding Properties of a Thiolated .beta.-Cyclodextrin Derivative. *J. Am. Chem. Soc.* **1995**, *117*, 336–343.

(20) Kitano, H.; Taira, Y.; Yamamoto, H. Inclusion of Phthalate Esters by a Self-Assembled Monolayer of Thiolated Cyclodextrin on a Gold Electrode. *Anal. Chem.* **2000**, *72*, 2976–2980.

(21) Filippini, G.; Bonal, C.; Malfreyt, P. Why is the Association of Supramolecular Assemblies Different Under Homogeneous and Heterogeneous Conditions? *Phys. Chem. Chem. Phys.* **2012**, *14*, 10122–10124.

(22) Pensa, E.; Cortes, E.; Corthey, G.; Carro, P.; Vericat, C.; Fonticelli, M. H.; Benitez, G.; Rubert, A.; Salvarezza, R. C. The Chemistry of the Sulfur Gold Interface: In Search of a Unified Model. *Acc. Chem. Res.* **2012**, *45*, 1183–1192.

(23) Torres, E.; Biedermann, P. U.; Blumenau, A. T. The Role of Gold Adatoms in Self-Assembled Monolayers of Thiol on Au(111). *Int. J. Quantum Chem.* **2009**, *109*, 3466–3472.

(24) Paulius, D.; Torres, D.; Illas, F.; Archibalda, W. E. A Study on Adatom Transport Through $(\sqrt{3} \times \sqrt{3})$–R30 °–CH3S Self-Assembled Monolayers on Au(111) Using First Principles Calculations. *Phys. Chem. Chem. Phys.* **2014**, *16*, 23067–23073.

(25) Whetten, R. L.; Price, R. C. Nano-Golden Order. *Science* **2007**, *318*, 407–408.

(26) Häkkinen, H. The Gold–Sulfur Interface at the Nanoscale. *Nat. Chem.* **2012**, *4*, 443–455.

(27) Zojer, E.; Taucher, T. C.; Hofmann, O. T. The Impact of Dipolar Layers on the Electronic Properties of Organic/Inorganic Hybrid Interfaces. *Adv. Mater. Interfaces* **2019**, *6*, 1900581.

(28) Rissner, F.; Rangger, G. M.; Hofmann, O. T.; Track, A. M.; Heimel, G.; Zojer, E. Understanding the Electronic Structure of Metal/SAM/Organic-Semiconductor Heterojunctions. *ACS Nano* **2009**, *3*, 3513–3520.

(29) Burshtain, D.; Mandler, D. The Effect of Surface Attachment on Ligand Binding: Studying the Association of Mg^{2+} , Ca^2+ and Sr^{2+} by 1-Thioglycerol and 1,4-Dithiothreitol Monolayers. *Phys. Chem. Chem. Phys.* **2006**, *8*, 158–164.

(30) Liu, Y.; Guo, D. S.; Zhang, H. Y.; Ma, Y. H.; Yang, E. C. The Structure and Thermodynamics of Calix[n]arene Complexes with Dipyridines and Phenanthroline in Aqueous Solution Studied by Microcalorimetry and NMR Spectroscopy. *J. Phys. Chem. B* **2006**, *110*, 3428–3434.

(31) Arena, G.; Casnati, A.; Contino, A.; Lombardo, G. G.; Sciotto, D.; Ungaro, R. Water-Soluble Calixarene Hosts that Specifically Recognize the Trimethylammonium Group or the Benzene Ring of Aromatic Ammonium Cations: A Combined 1H NMR, Calorimetric, and Molecular Mechanics Investigation. *Chem. Eur. J.* **1999**, *5*, 738–744.

(32) Goujon, F.; Bonal, C.; Limoges, B.; Malfreyt, P. Molecular Simulations of Grafted Metal-Chelating Monolayers: Methodology, Structure and Energy. *Mol. Phys.* **2008**, *106*, 1397–1411.

(33) Abascal, J. L. F.; Vega, C. A General Purpose Model for the Condensed Phases of Water: TIP4P/2005. *J. Chem. Phys.* **2005**, *123*, 234505.

(34) Wang, J.; Wolf, R. M.; Caldwell, J. W.; Kollman, P. A.; Case, D. A. Development and Testing of a General Amber Force Field. *J. Comput. Chem.* **2004**, *25*, 1157–1174.

(35) Heinz, H.; Vaia, R. A.; Koerner, H.; Farmer, B. L. Photoisomerization of Azobenzene Grafted to Layered Silicates: Simulation and Experimental Challenges. *Chem. Mater.* **2008**, *20*, 6444–6456.

(36) Rai, B.; Sathish P.,; Malhotra, C. P.; Pradip,; Ayappa, K. G. Molecular Dynamic Simulations of Self-Assembled Alkylthiolate Monolayers on an Au(111) Surface. *Langmuir* **2004**, *20*, 3138–3144.

(37) Plimpton, S. Fast Parallel Algorithms for Short-Range Molecular Dynamics. *J. Comput. Phys.* **1995**, *117*, 1–19.

(38) Ryckaert, J.-P.; Ciccotti, G.; Berendsen, H. J. C. Numerical Integration of the Cartesian Equations of Motion of a System with Constraints: Molecular Dynamics of n-Alkanes. *J. Comput. Phys.* **1977**, *23*, 327–341.

(39) Schneider, T.; Stoll, E. Molecular-Dynamics Study of a Three-Dimensional One-Component Model for Distortive Phase Transitions. **1978**,

(40) Dünweg, B.; Paul, W. Brownian Dynamics Simulations Without Gaussian Random Numbers. **1991**,

(41) Sun, H. COMPASS: An ab Initio Force-Field Optimized for Condensed-Phase Applications Overview with Details on Alkane and Benzene Compounds. *J. Phys. Chem. B* **1998**, *102*, 7338–7364.

(42) Hockney, R. W.; Eastwood, J. W. *Computer Simulation Using Particles*; CRC Press, 1988.

(43) Pollock, E. L.; Glosli, J. Comments on P3M, FMM, and the Ewald Method for Large Periodic Coulombic Systems. *Comput. Phys. Commun.* **1996**, *95*, 93–110.

For Table of Contents Only